Accelerated CEST MRI using parallel imaging acquisition of golden-angle radial ordering scheme and compressed sensing reconstruction

Jinsuh Kim[1], Casey P Johnson[2], Dingxin Wang[3], and Philip Zhe Sun[4]
[1]University of Iowa, Iowa City, IA, United States, [2]University of Iowa, IA, United States, [3]Siemens Medical Solutions USA, Inc., Minneapolis, MN, United States, [4]Martinos Center for Biomedical Imaging, MGH, Charlestown, MA, United States

Introduction

CEST imaging sequence typically includes lengthy RF saturation irradiation preparations that are repeated over a range of frequencies. For this reason, it inherently requires long scanning time which has significantly hampered its clinical translation. In general, conventional imaging sequences with full Cartesian k-space sampling are less suitable to achieve high resolution Z-spectral acquisition within a practical scanning time limit. Compressed sensing (CS) image reconstruction from sparsely undersampled k-space data beyond the Nyquist sampling limit can be further improved with parallel imaging technique and incoherent sampling achieved by the golden-angle (GA) ordering scheme; i.e., a radial trajectory with an angular increment of 111.25° or 68.75° [1,2]. In this work, we introduce an accelerated CEST imaging using a GA-radial CS method and provide a proof-of-concept of the new method for future clinical employment.

Method

All measurements were performed on a Siemens 3T system with an extremity coil in a creatine (Cr) phantom, and the right lower leg of a volunteer subject. The phantom consisted of 4 tubes of Cr solution with titrated pH 6.5 and concentration of 50, 75, 100, and 125 mM within a water-filled container doped with trace of $MnCl_2$. The CEST images were acquired with a radial FLASH sequence through 16 parallel imaging channels. Saturation irradiation consisted of 10 pulsed-train of 25 ms Gaussian RF pulses with 50% duty cycle, swept between ± 3 ppm. To validate *in vivo* application of GA-radial ordering method, CEST scans on the lower leg were performed at baseline (pre-exercise), after 5 min period of plantar flexion ankle exercise (post-exercise), and after 10 min resting using following parameters: TR/TE=680/2.6 msec, slice thickness=5 mm, matrix=128x128, FoV=180 mm. The exercise-induced changes of Cr CEST effect were compared at each phase. Radial trajectory schemes were: (A) conventional 10 rotated radial spokes per frame and conjugate gradient (CG) SENSE reconstruction, and (B) continuous GA rotations (68.75° angular increment) with fine consecutive increment of saturation offset frequencies for each radial spoke, subsequently reconstructed by prior image constrained compressed sensing (PICCS) method [3]. Iterative reconstruction algorithm (Split-Bregman) solved minimization problem of the energy function with L1 and L2-regularization terms as: $\mu = \arg\min_{\mu} \alpha \|\mu\|_{TV} + \beta \|\Phi\mu\|_1 + \lambda \|A\mu - y\|_2^2$. Image reconstructions were performed on a computer with GPGPU-enabled Gadgetron framework [4]. Real-time image reconstruction results were transported to the MRI system over Ethernet connection. The SNR efficiency was expressed as SNR per-unit-time: $SNR_{put} = \frac{CESTR/\sigma}{\sqrt{TR \cdot NEX}}$ [5].

Result

Fig. 1 shows CESTR maps from the Cr phantom; 10 radial spokes per frame with CG-SENSE reconstruction (scheme A), and GA radial acquisitions with reconstruction of 8 spokes per frame using CS method (scheme B). Scanning times for 5 slice images of the scheme A and B were 24 min and 13 min respectively. CESTR values (%) at 1.8 ppm of 75 mM Cr phantom were 6.1±1.1 (mean±S.D.) in scheme A and 10.1±1.9 in scheme B. SNR_{put} of the scheme A and B were estimated at 1.34 and 1.01 respectively, which account for more residual streaking artifacts in the scheme B. However saturation images of the scheme A demonstrated significant edge blurring with poor point spread function profile when compared to those of the scheme B. Cr CESTR(%) measured from the calf muscle ROI at pre, post-exercise and after-resting were 0.22, 3.89, and 2.53 respectively (Fig. 2).

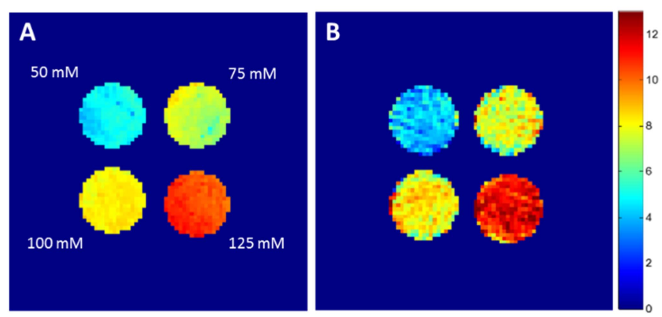

Fig. 1. Creatine CESTR maps. (A) 10 radial spokes per frame with CG-SENSE reconstruction, (B) GA-radial scheme with CS reconstruction.

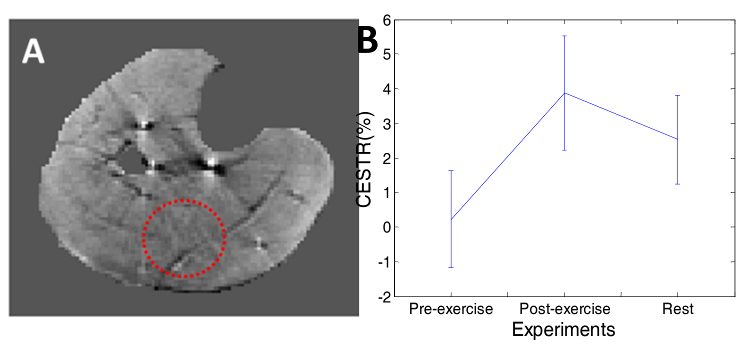

Fig. 2. (A) Pre-exercise Cr CESTR map and defined ROI (red dotted circle), (B) Plot of exercise-induced Cr CESTR changes measured at ROIs.

Discussion

GA-radial method enabled highly accelerated CEST image acquisition with enhanced CEST sensitivity. Practical feasibility of this method is corroborated by *in vivo* Cr CEST experiments in the lower leg. CS reconstruction effectively reduced streak artifacts of GA-radial scheme producing excellent quality of output images on visual inspection. However the SNR efficiency of resultant CEST map from the GA-radial scheme was slightly worse than the conventional radial scheme. Quality of CEST map can be further improved with improved RF saturation strategies and optimized regularization of CS reconstruction.

Reference

[1] Sorensen TS, et al., IEEE TMI 28:1974-85 (2009). [2] Feng L, et al., MRM 69:1768-76 (2013). [3] Chen GH, et al., Med Phys 35(2):660-3 (2008). [4] Hansen MS, et al., MRM 69:1768-76 (2013). [5] Sun PZ, et al., Phys Med Biol 58(17):N229-40 (2013).